

# Upgrading of Trimethylolpropane Oleate to Biojet Fuel Range Hydrocarbons Through Catalytic Deoxygenation

Jianxin Zhang<sup>a</sup>, Brandon Han Hoe Goh<sup>a</sup>, Jo-Han Ng<sup>b</sup>, Cheng Tung Chong<sup>a,\*</sup>

<sup>a</sup>China-UK Low Carbon College, Shanghai Jiao Tong University, Lingang, Shanghai 201306, China.

<sup>b</sup>Carbon Neutrality Research Group, University of Southampton Malaysia, 79100 Iskandar Puteri, Johor, Malaysia  
 ctchong@sjtu.edu.cn

Utilising non-hydrogen environments to convert fatty acids to liquid fuels is potentially an economical, green and promising method for sustainable fuel production. This work focuses on solvent-free biojet fuel generation (C8 to C16) from the trimethylolpropane oleate (TMPE) using transition metal-loaded TiO<sub>2</sub> as a solid acid catalyst. Wet impregnation was implemented to produce a series of TiO<sub>2</sub>-based cobalt, nickel, and iron catalysts with 2 wt.% metal loading without reduction. Each catalyst was tested for the deoxygenation of TMPE at 350 °C for 2 h at atmospheric pressure in a N<sub>2</sub> atmosphere. It was found that using transition metal catalysts without reduction in a non-hydrogen environment could generate hydrocarbons with carbon chain lengths within the jet fuel range. The abundance of acid sites on the Fe catalyst helps break C-O bonds and facilitate the deoxygenation process. Fe/TiO<sub>2</sub> exhibited the highest selectivity for C8 to C16 hydrocarbons (53.7 %) with relatively good deoxygenation performance (74.2 %). Although impregnation of transition metals resulted in reduction of specific surface area, the additional active sites were able to promote deoxygenation and breaking bond reactions to occur. The acidic sites provided by Fe metal and TiO<sub>2</sub> carriers indicate that the catalyst is suitable for atmospheric nitrogen deoxygenation of TMPE for the preparation of biojet fuel. The result shows the potential of using a non-hydrogen environment to perform deoxygenation on long-chain fatty acid molecules to derive jet-fuel range hydrocarbons.

## 1. Introduction

As the international air transportation industry grows, the impact of greenhouse gas emissions from conventional fossil aviation fuels is increasingly of concern. Compared to ground transportation, air transportation is characterised by long transport distances, high power and the inability to replenish energy sources midway (Monteiro et al., 2022). This means that aircraft electrification is not an option, as the energy density of a battery is no match for fossil jet fuel. Other alternative energy systems, such as solar, hydrogen and fuel cells, are unable to meet the power requirements of aircraft flight. Currently, the viable way to replace jet fuel is through the use of, biojet fuels prepared from biomass, such as animal fats, plant oils, agricultural waste, which have comparable jet fuel properties and significant emission reduction characteristics. Triglycerides are the main components of oils consisting of a glycerol backbone and three long-chain fatty acids. It is prospective for conversion to hydrocarbons in the biojet range (C8–C16) (Max Romero, 2018). Since biojet fuels can seamlessly blend with existing fossil jet fuels to achieve good compatibility with aircraft, aviation engines and aviation fuel supply systems, they have become an excellent choice for aviation decarbonisation (Li et al., 2024).

Biojet fuel is a complex mixture of mainly C8-C16 hydrocarbons, which varies according to the source of crude oil and the manufacturing process. The preparation of C8-C16 length hydrocarbons can be achieved through processes such as bond breaking and isomerisation, where metal-acidic bifunctional catalysts enable these two processes to occur simultaneously (Zulkepli et al., 2022). TMPE contains three ester groups where all three branched chains are saturated carbon chains, making it an excellent raw material for biojet fuel production. Biojet fuel hydrocarbons can be produced from oxygenated fats and oils by undergoing decarbonylation (DCO), decarboxylation (DCO<sub>2</sub>), or hydrodeoxygenation (HDO) processes (Hongloi et al., 2022). The HDO process consumes more hydrogen, whereas DCO and DCO<sub>2</sub> consume less hydrogen but produce CO and CO<sub>2</sub>, resulting

in a loss of carbon. Different types of transition metal-based catalysts and carriers can facilitate different deoxygenation routes. The design of catalysts with appropriate physicochemical properties is important to obtain highly selective products and to reduce side reactions (Zhou et al., 2023).

In the preparation of biojet fuel, the addition of catalysts significantly enhances the DCO<sub>2</sub>, DCO and HDO processes during deoxygenation of waste cooking oil (Razak et al., 2024). However, catalysts are prone to problems such as deactivation during the catalytic reaction. The effective catalyst design is needed to improve the catalyst activity and the number of active sites for regulating the distribution of catalytic products. Acidic sites on the Fe, Co, and Ni catalysts help to break the C-O bond and facilitate the deoxygenation process by adsorbing and activating lipid molecules, which increase the reaction rate and selectivity (Serrer et al., 2020). Typically, TiO<sub>2</sub> loaded with transition metals, facilitates the conversion of fats and oils to hydrocarbons in the range of jet fuels from the synergistic effect. In addition, transition metal (Co, Ni and Fe) loaded catalysts were effective in reducing the number of oxygenates and promoting the generation of hydrocarbons (Zhang et al., 2022). Lin et al. (2020) investigated the reaction principle of pyrolysis of cedar wood and low-density polyethylene using Fe-loaded activated carbon catalysts to produce biojet fuel hydrocarbons. The incorporation of Fe enhanced hydrogen transfer and facilitated the dehydroxylation and demethoxylation in the phenolics. The preparation of transition metal catalysts using a one-step process is simple and can be retrofitted into existing petroleum engineering facilities to increase the possibility of industrialisation compared to other preparation processes. Currently, Fe, Co and Ni catalysts have lower costs than precious metal catalysts (e.g., Pt, Pd, etc.), providing economic advantages in large-scale industrial applications. In this paper, the effect of using transition metal bifunctional catalysts on the deoxygenation performance of TMPE was analysed. The catalysts were formed by combining Ni, Co, Fe and TiO<sub>2</sub> using the wet method which were analysed on the basis of morphology, chemical elements and specific surface area. The deoxygenation performance of TMPE was evaluated based on the production of hydrocarbons in the C8-C16 range.

## 2. Materials and Methods

### 2.1 Catalyst preparation

Nickel, cobalt, iron catalysts were prepared using a non-reduced impregnation method. The use of high temperature calcination under inert gas atmosphere can effectively activate the catalyst while avoiding the introduction of hydrogen. Utilizing 2 g of metal nitrate hexahydrate dissolved in deionised water using magnetic stirring for 1 h and then mixed with TiO<sub>2</sub> carrier. Dry in an oven at 100°C for 12 h. The dried mixture was calcined in a tube furnace at 350°C with a ramp rate of 8°C/min and a holding time of 4 h to promote decomposition of the compounds (Goh et al., 2023). After calcination the catalyst was cooled to room temperature and ground into uniform particles using a mortar and pestle.

### 2.2 Catalyst characterisation

Morphological structure and elemental composition of the catalysts were characterised by Scanning Electron Microscopy (SEM) coupled with Energy X-ray Spectroscopy (EDS). Brunauer-Emmet-Teller (BET) method was used to determine the specific surface area of the catalysts, while the pore size distribution of the catalysts was calculated based on isothermal adsorption branching using Barrett-Joyner-Halenda (BJH) method. The elemental composition was further determined by X-ray fluorescence analysis using the Axios Max instrument.

### 2.3 Deoxygenation procedure for TMPE

The deoxygenation of TMPE was carried out in an inert environment and heated in a 250 mL three-necked flask. The flow rate of N<sub>2</sub> was accurately controlled at 200 mL/min using a mass flow meter. 100 g of TMPE feedstock and 5 g of catalyst were added simultaneously to the three-necked flask. N<sub>2</sub> was introduced for 5 min to purge the air from the three-necked flask. After 5 min, the reaction was started with heating and stirring at a speed of 300 r/min and a heating temperature of 350 °C. Heating of the reaction with a thermostatic magnetic stirrer (Shanghai Li-Chen Technology Co., SCZL 500 mL). The reaction time was 2 h. The whole setup was cooled to room temperature in an N<sub>2</sub> environment. The products from the reaction were carried by the N<sub>2</sub> flow into the condensation tube and collected in a collection bottle the temperature changed. The products after deoxygenation were mainly analysed using gas chromatography. The performance of TMPE deoxygenation and hydrocarbon selectivity were evaluated based on chromatographic peak area calculations. The analysis is based on the relative content of each substance, which is proportional to the peak area. The deoxygenation performance and selectivity were obtained using GC-MS data as follows:

$$\text{Deoxygenation performance} = \frac{\text{Alkane peak area} + \text{Alkene peak area}}{\text{Total peak area}} \times 100 \% \quad (1)$$

$$\text{Hydrocarbon selectivity} = \frac{\text{Total hydrocarbon peak area in the C8-C16 range}}{\text{Total peak area}} \times 100 \% \quad (2)$$

### 3. Results and Discussion

The morphological structure of  $\text{TiO}_2$ ,  $\text{Ni/TiO}_2$ ,  $\text{Co/TiO}_2$  and  $\text{Fe/TiO}_2$  are shown in Figure 1. Figure 1 (a-d), the surface morphologies of these different catalysts at various magnifications. The four catalysts exhibit a spherical stacking structure with relatively uniform particle size. The introduction of metal particles did not alter the carrier structure. The structure of the catalyst did not show collapse or change, proving that the high temperature did not greatly affect the structure.

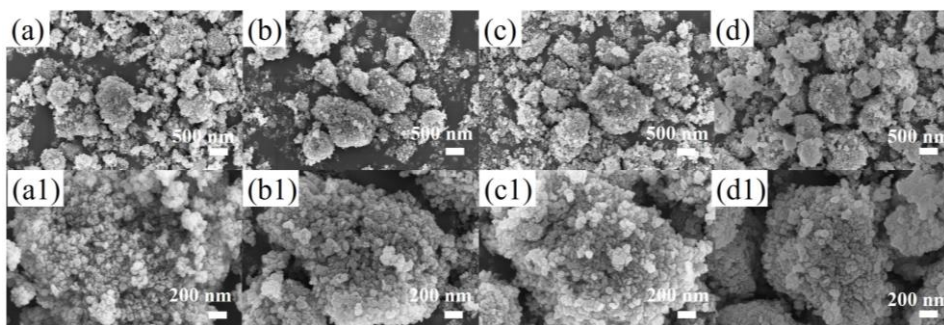


Figure 1: SEM of (a-a1)  $\text{TiO}_2$ ; (b-b1)  $\text{Ni/TiO}_2$ ; (c-c1)  $\text{Co/TiO}_2$ ; (d-d1)  $\text{Fe/TiO}_2$  catalysts.

EDS shown the presence of Ti, O and Fe (Ni or Co) indicating successful metal impregnation on the carrier (Figure 2). Notably, the purple and orange point distributions observed in the EDS images indicate successful and uniform attachment of Fe (Ni or Co) to the  $\text{TiO}_2$  carrier, which is beneficial for efficient catalysis. However, the vague profile of the Fe (Ni and Co) elements are mainly due to the doping amounts being only 2 wt.%.

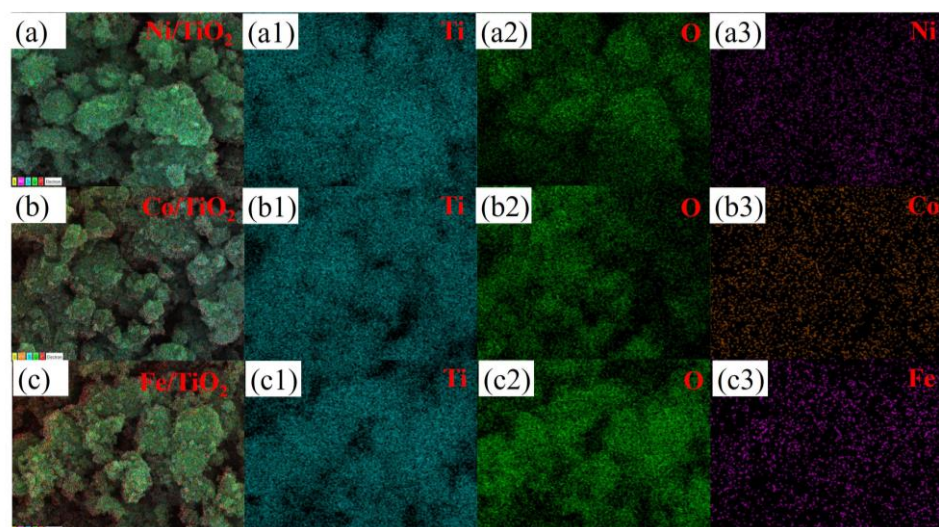


Figure 2: EDS of (a-a3)  $\text{Ni/TiO}_2$  Ti, O, Ni; (b-b3)  $\text{Fe/TiO}_2$  Ti, O, Co; (c-c3)  $\text{Fe/TiO}_2$  Ti, O, Fe.

The specific surface area and XRF elemental analysis of different catalysts were analysed (Table 1). It shows that pure  $\text{TiO}_2$  has the largest specific surface area, which decreases with the addition of transition metals. In Table 1, the specific surface area and pore volume increased with the addition of transition metal, indicating that the introduction of metal particles has a significant effect on the improvement of the void structure, which makes it easier to expose the active sites in the catalyst and improve the catalytic performance. However, the difference in the specific surface area of the catalysts with the introduction of transition metals is minimal. Characterisation using XRF showed that  $\text{NiO}$ ,  $\text{Co}_3\text{O}_4$  and  $\text{Fe}_2\text{O}_3$  were the main components in the catalyst.  $\text{TiO}_2$  retains its original chemical composition after high temperature. The mass percentages of  $\text{NiO}$ ,  $\text{Co}_3\text{O}_4$  and  $\text{Fe}_2\text{O}_3$  after activation were 5.167, 3.99, and 4.994. It is evident that the ratio of transition metals in the  $\text{TiO}_2$  carrier did not significantly change after activation, which demonstrates that the transition metals were successfully activated without compromising the structure of  $\text{TiO}_2$ .

Table 1: Composition and pore distribution of catalysts.

Catalyst	Specific surface area (m <sup>2</sup> /g)	Average pore diameter (nm)	Pore volume (cm <sup>3</sup> /g)	TiO <sub>2</sub> (wt%)	NiO (wt%)	Co <sub>3</sub> O <sub>4</sub> (wt%)	Fe <sub>2</sub> O <sub>3</sub> (wt%)
TiO <sub>2</sub>	96.51	0.352	2.375	97.3	-	-	-
Ni/TiO <sub>2</sub>	64.215	0.312	14.880	93.185	5.167	-	-
Co/TiO <sub>2</sub>	68.800	0.262	12.337	93.042	-	4.971	-
Fe/TiO <sub>2</sub>	67.422	0.307	15.123	93.658	-	-	4.994

NH<sub>3</sub>-TPD was used to study the distribution of acid sites on the catalyst surface, and all four catalysts showed weakly acidic sites (Figure 3). Acid strength is significantly increased with the addition of metal elements. The introduction of Ni, Co, and Fe metals can interact with surface oxides to form new Lewis acidic sites (Xia et al., 2022). The Fe/TiO<sub>2</sub> exhibits the strongest acidity (NH<sub>3</sub> resolution at 456 °C). The type of active metal directly affects the acidity of the catalysts, and this may be related to the fact that Brønsted acidic sites and Lewis acidic sites can be present on the catalyst surface. The presence of acidic sites and metal active sites play an important role in TMPE cracking, while metal active sites can promote the deoxygenation reaction. Acidic sites can promote TMPE to undergo cracking, which promotes the Fe/TiO<sub>2</sub> to exhibit excellent C8-C16 selectivity.

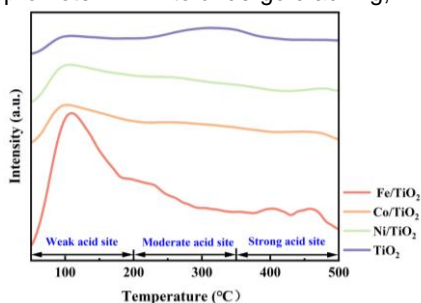
Figure 3. NH<sub>3</sub>-TPD profile of TiO<sub>2</sub>, Ni/TiO<sub>2</sub>, Co/TiO<sub>2</sub>, Fe/TiO<sub>2</sub>.

Figure 4 illustrates the product distribution after the deoxygenation reaction. The products of Fe/TiO<sub>2</sub>-catalysed pyrolysis consisted primarily of alkanes, achieving a deoxygenation performance of 74.2 %. In contrast, the products of Ni/TiO<sub>2</sub> and Co/TiO<sub>2</sub>-catalysed pyrolysis were mainly alkenes, with deoxygenation performance of 58.8 % and 57.7 %. This shows that catalysts containing Fe have significant potential for producing hydrocarbons within the biojet fuel range. In the environment of N<sub>2</sub>, Fe/TiO<sub>2</sub> showed attractive deoxygenation performance. Fe catalysts are known for their oxyphilic nature, which helps in the adsorption and activation of oxygenated compounds. This property enhances the deoxygenation process by facilitating the removal of oxygen atoms from the feedstock (Zhang et al., 2021). Zhang et al. utilized a Ce@Fe@SAPO-34 catalyst to selectively dehydrate low carbon alcohols or ABE (acetone/butanol/ethanol) to form light alkenes. High ABE conversion (89.3 %) and jet fuel yield (71.5 %) were achieved by a two-step coupling process at atmospheric pressure. In the absence of an external source of hydrogen, TMPE will first undergo hydrolysis to form alcohols and unsaturated fatty acids, as evidenced by the presence of alcohol compounds in each product.

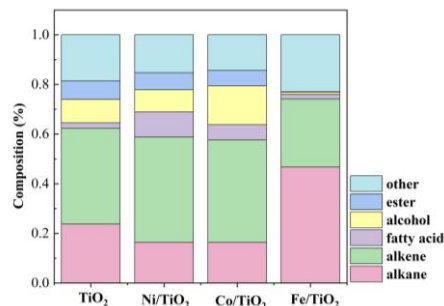
Figure 4: Composition of deoxygenated products for TiO<sub>2</sub>, Ni/TiO<sub>2</sub>, Co/TiO<sub>2</sub>, Fe/TiO<sub>2</sub>.

Figure 5 shows the percentage of hydrocarbons with different carbon chain lengths in the hydrocarbon product. From the Figure 5, it is evident that the C8-C16 hydrocarbons are consistently higher than the C4-C7 range

hydrocarbons, indicating that hydrocarbons in the jet fuel range are the main products. Among them, the selectivity of Fe/TiO<sub>2</sub> for hydrocarbons in the C8-C16 range is 57.3 %. The selectivity of Ni/TiO<sub>2</sub> and Co/TiO<sub>2</sub> for hydrocarbons in the C8-C16 range is 36.6 % and 40.9 %. The C8-C16 selectivity of the catalysts containing transition metal elements is consistently higher than that of TiO<sub>2</sub> at 36.0 %. This indicates that the selectivity of hydrocarbons in the jet fuel range has been improved. The results show that transition metal element-containing catalysts are significantly more selective for hydrocarbons in the jet fuel range than pure TiO<sub>2</sub>. It was demonstrated that the introduction of Ni element alone contributes little to improving the selectivity of the catalyst and this is consistent with the finding that Ni promotes isomerization (Xu et al., 2020).

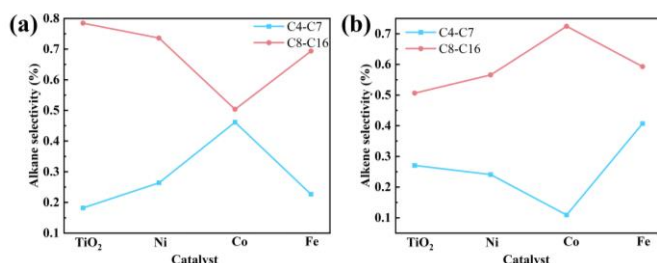


Figure 5: Carbon chain selectivity for (a) alkanes and (b) alkenes in the range of C4-C16 for different catalysts.

Figure 6 shows possible reaction pathways for the production of jet fuel range hydrocarbons by catalysts containing transition metal elements. Hydrolysis of TMPE to form unsaturated fatty acids and glycerol can occur using transition metal/TiO<sub>2</sub> catalysts under N<sub>2</sub> atmosphere at a reaction temperature of 350°C and a N<sub>2</sub> flow of 2 h. The presence of double bonds in TMPE, make the deoxygenation process of unsaturated esters more complex compared to saturated esters. In the absence of an external hydrogen source, unsaturated fatty acids can be directly decarboxylated or decarbonylated to form alkenes. The alkene requires a hydrogen atom to be hydrogenated to form an alkane, where the hydrogen atom can originate from a gas-phase reaction, catalyst or carrier (Asikin-Mijan et al., 2020). The ester groups may be converted into desirable jet fuel-grade hydrocarbons by cracking, DOC and DOC<sub>2</sub> processes. Overall, the Fe catalyst exhibits the highest activity. Firstly, Fe loaded on TiO<sub>2</sub> may promote C=O bond breaking (Sitthisa et al., 2011). Fe-loaded TiO<sub>2</sub> carriers with optimal acidic sites will also promote side reactions including DCO<sub>2</sub>, cracking, dehydrogenation and cyclization (Farooq et al., 2023). The uniform distribution of Fe on the carrier improves the activity of the catalyst. Based on the analysis of GC-MS data, the main products of the Fe/TiO<sub>2</sub>-catalysed reaction included heptane, octane, nonane, 1-heptane and cyclopropane, pentyl.

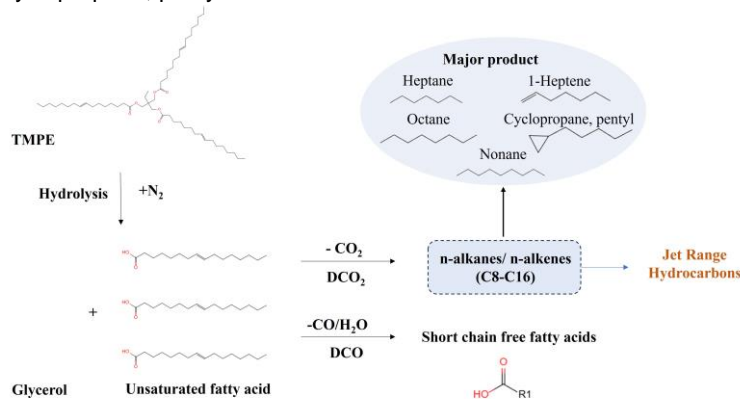


Figure 6: Schematic diagram of the reaction pathway for the Fe/TiO<sub>2</sub>-catalysed deoxygenation of TMPE.

#### 4. Conclusions

Currently, developing efficient catalysts for biojet fuel production necessitates stable catalysts that are selective for high high-purity products. Efficient catalysts also minimise feedstock waste while achieving high product yields. The effects of various transition metal catalysts on the deoxygenation of oxygen-containing TMPE were analysed. The focus of this study was on the production of biojet fuels using long-chain oxygenated oils as feedstock, catalysed by transition metal/TiO<sub>2</sub> catalysts in an N<sub>2</sub> environment. The effect of Ni, Co and Fe catalysts on the deoxygenation of TMPE were systematically investigated under identical reaction conditions.



The synergistic effect of Fe on nano-TiO<sub>2</sub> increased the deoxygenation efficiency and selectivity of C<sub>8</sub>-C<sub>16</sub> hydrocarbons to 74.2 % and 57.3 % It was found that Fe exhibits excellent deoxygenation capabilities, highlighting that different transition metals interacts differently with oxygen-containing functional groups. Additionally, varying the use of N<sub>2</sub> in the deoxygenation process is crucial for reducing reliance on H<sub>2</sub> in the hydrodeoxygenation process.

### Acknowledgments

The authors would like to thank for the financial support from the research fund for International Excellent Young Scientists (52250610220) awarded by the National Natural Science Foundation of China (NSFC).

### References

- Monteiro R.R.C., da Silva S.S.O., Cavalcante C.L., Jr., de Luna F.M.T., Bolivar J.M., Vieira R.S., Fernandez-Lafuente R., 2022, Biosynthesis of alkanes/alkenes from fatty acids or derivatives (triacylglycerols or fatty aldehydes). *Biotechnology Advances*, 61, 108045.
- Max Romero A.P., Giuseppe Toscanob, Alessandro Alberto Casazzaa, Guido Buscaa, Barbara Bosioa, Elisabetta Aratoa., 2018, Deoxygenation of Non-Edible Vegetable Oil to Produce Hydrocarbons Over Mg-Al Mixed Oxides. *Chemical Engineering Transactions*, 64,121-126.
- Li D.C., Pan Z., Tian Z., Zhang Q., Deng X., Jiang H., Wang G.H., 2024, Frustrated Lewis pair catalyst realizes efficient green diesel production. *Nature Communications*, 15(1), 3172.
- Razak N.A.A., Taufiq-Yap Y.H., Derawi D., 2024, Catalytic deoxygenation of waste cooking oil for sustainable bio-jet fuel: A comparative study of Ni-Co/SBA-15 and Ni-Co/SBA-15-SH catalysts. *Journal of Analytical and Applied Pyrolysis*, 178, 106369.
- Zulkepli S., Abd. Rahman N., Voon Lee H., Kui Cheng C., Chen W.-H., Ching Juan J., 2022, Synergistic effect of bimetallic Fe-Ni supported on hexagonal mesoporous silica for production of hydrocarbon-like biofuels via deoxygenation under hydrogen-free condition. *Energy Conversion and Management*, 273, 116371.
- Hongloi N., Prapainainar P., Prapainainar C., 2022, Review of green diesel production from fatty acid deoxygenation over Ni-based catalysts. *Molecular Catalysis*, 523, 111696.
- Zhou Y., Remón J., Jiang Z., Matharu A.S., Hu C. W., 2023, Tuning the selectivity of natural oils and fatty acids/esters deoxygenation to biofuels and fatty alcohols: A review. *Green Energy & Environment*, 8(3), 722-743.
- Serrer M.-A., Gaur A., Jelic J., Weber S., Fritsch C., Clark A.H., Saraçi E., Studt F., Grunwaldt J.-D., 2020, Structural dynamics in Ni-Fe catalysts during CO<sub>2</sub> methanation – role of iron oxide clusters. *Catalysis Science & Technology*, 10(22), 7542-7554.
- Zhang Z., Tian J., Lu Y., Gou X., Li J., Hu W., Lin W., Kim R.S., Fu J., 2022, Exceptional Selectivity to Olefins in the Deoxygenation of Fatty Acids over an Intermetallic Platinum-Zinc Alloy. *Angewandte Chemie-International Edition*, 61(18), e202202017.
- Lin X., Lei H., Huo E., Qian M., Mateo W., Zhang Q., Zhao Y., Wang C., Villota E., 2020, Enhancing jet fuel range hydrocarbons production from catalytic co-pyrolysis of Douglas fir and low-density polyethylene over bifunctional activated carbon catalysts. *Energy Conversion and Management*, 211, 112757.
- Goh B.H.H., Chong C.T., Ng J.-H., 2023, Hydrogen-free Deoxygenation of Waste Cooking Oil over Unreduced Bimetallic NiCo Catalysts for Biojet Fuel Production. *Chemical Engineering Transactions*, 106, 721-726.
- Zhang L., Dang Y., Zhou X., Gao P., Petrus van Bavel A., Wang H., Li S., Shi L., Yang Y., Vovk E.I., 2021, Direct conversion of CO<sub>2</sub> to a jet fuel over CoFe alloy catalysts. *Innovation (Camb)*, 2(4), 100170.
- Xia, S.P., Wang, C.Y., Chen, Y., Kang, S.S., Zhao, K., Zheng, A.Q., Zhao, Z.L., Li, H.B., 2022, Sustainable Aromatic Production from Catalytic Fast Pyrolysis of 2-Methylfuran over Metal-Modified ZSM-5. *Catalysts*, 12, 1483.
- Xu Y.P., Wang Z.Q., Tan H.Z., Jing K.Q., Xu Z.N., Guo G.C., 2020, Lewis acid sites in MOFs supports promoting the catalytic activity and selectivity for CO esterification to dimethyl carbonate. *Catalysis Science & Technology*, 10(6), 1699-1707.
- Asikin-Mijan N., Ooi J.M., AbdulKareem-Alsultan G., Lee H.V., Mastuli M.S., Mansir N., Alharthi F.A., Alghamdi A.A., Taufiq-Yap Y.H., 2020, Free-H<sub>2</sub> deoxygenation of *Jatropha curcas* oil into cleaner diesel-grade biofuel over coconut residue-derived activated carbon catalyst. *Journal of Cleaner Production*, 249, 119381.
- Sitthisa S., An W., Resasco D.E., 2011, Selective conversion of furfural to methylfuran over silica-supported NiFe bimetallic catalysts. *Journal of Catalysis*, 284(1), 90-101.
- Farooq A., Shuing Lam S., Jae J., Ali Khan M., Jeon B.-H., Jung S.-C., Park Y.-K., 2023, Jet fuel-range hydrocarbons generation from the pyrolysis of saw dust over Fe and Mo-loaded HZSM-5(38) catalysts. *Fuel*, 333, 126313.